



**HAL**  
open science

# ASSESSING BI-STABLE VENTILATION FOR SURFACE-PIERCING HYDROFOILS THROUGH NUMERICAL SIMULATION

M Charlou, Jeroen Wackers, G.B. Deng, Emmanuel Guilmineau, Alban  
Leroyer, Patrick Queutey, Michel Visonneau

► **To cite this version:**

M Charlou, Jeroen Wackers, G.B. Deng, Emmanuel Guilmineau, Alban Leroyer, et al.. ASSESSING BI-STABLE VENTILATION FOR SURFACE-PIERCING HYDROFOILS THROUGH NUMERICAL SIMULATION. Innov'Sail 2020, Jun 2020, Goteborg, Sweden. hal-02571240

**HAL Id: hal-02571240**

**<https://hal.science/hal-02571240>**

Submitted on 12 May 2020

**HAL** is a multi-disciplinary open access archive for the deposit and dissemination of scientific research documents, whether they are published or not. The documents may come from teaching and research institutions in France or abroad, or from public or private research centers.

L'archive ouverte pluridisciplinaire **HAL**, est destinée au dépôt et à la diffusion de documents scientifiques de niveau recherche, publiés ou non, émanant des établissements d'enseignement et de recherche français ou étrangers, des laboratoires publics ou privés.

# ASSESSING BI-STABLE VENTILATION FOR SURFACE-PIERCING HYDROFOILS THROUGH NUMERICAL SIMULATION

**M. Charlou**, LHEEA, EC Nantes / CNRS, France, moran.charlou@ec-nantes.fr.

**J. Wackers**, LHEEA, EC Nantes / CNRS, France, jeroen.wackers@ec-nantes.fr.

**G.B. Deng**, LHEEA, EC Nantes / CNRS, France, ganbo.deng@ec-nantes.fr.

**E. Guilmineau**, LHEEA, EC Nantes / CNRS, France, emmanuel.guilmineau@ec-nantes.fr.

**A. Leroyer**, LHEEA, EC Nantes / CNRS, France, alban.leroyer@ec-nantes.fr.

**P. Queutey**, LHEEA, EC Nantes / CNRS, France, patrick.queutey@ec-nantes.fr.

**M. Visonneau**, LHEEA, EC Nantes / CNRS, France, michel.visonneau@ec-nantes.fr.

This paper studies the inception and stability of ventilation in bi-stable conditions. It is shown that spontaneous inception depends on the path to the steady state. Therefore, it is more relevant to provoke ventilation by artificial perturbation and to consider its stability, than to simulate spontaneous inception. At low angles of attack, the simulated ventilation is eliminated by a wave crest breaking and closing the ventilation pocket from the top. The tests show that this behaviour depends on the detailed physical and numerical modelling of the water sheet which forms the edge of the ventilating pocket.

## NOMENCLATURE

Symbol	Definition	(unit)
$\alpha$	Angle of attack / yaw	( rad. )
$\sigma$	Surface tension	( $\text{N.m}^{-1}$ )
$c$	Chord length	( m )
$Fn_h$	Immersion-based Froude number	( - )
$h$	Immersion depth	( m )
$t$	Physical time	( s )
$U_\infty$	Inflow velocity	( $\text{m.s}^{-1}$ )

## 1 INTRODUCTION

Most modern sea-faring vessels, regardless of their size, use lifting devices for both propulsion and control: sails, rudders and propeller blades are the most common instances. Furthermore, in sailing, lifting hydrofoils as a means of drag reduction have caused a jump in yacht performance over the recent years. For these foils, which are immersed but operate close to the free surface, there is a risk that the low pressure on the suction side entrains air from above the water. This phenomenon is called ventilation, and causes a drastic reduction of the lift force on the foil, as well as a possible reduction of the drag force. The drag reduction can be beneficial, but ventilation is usually a dangerous condition on a lifting device: it can lead to a loss of performance, a loss of control, or even to violent water impact which may lead to the destruction of a foiling yacht. The ventilated state can be transient if the flow goes back rapidly to the non-ventilated operational state, but it can also persist as a stable state.

In order to avoid the occurrence of ventilation on an immersed lifting device, it is useful to predict which specific flow con-

ditions are prone to ventilation. The flow around a surface-piercing hydrofoil is complex, since it may feature recirculation bubbles, trailing vortices, large pressure gradients, and steep surface depressions. A numerical study of such a flow must be able to simulate all of these features accurately because they may all play a role in ventilation phenomena.

On a surface-piercing lifting hydrofoil at high Froude numbers, wetted flow occurs when water covers both sides of the foil completely, while ventilated flow implies that a pocket of air covers a major part of the suction side. The flow is often wetted for low angles of attack and ventilated at high angles. However, there is a range of angles in between, where both flow regimes exist and are stable. In this bi-stable region, a perturbation can brutally change the flow from wetted to ventilated and conversely. The flow regime cannot be determined by the conditions only: its history must be considered as well. A review of these phenomena is presented by Young et al. [6].

Harwood et al. [2, 3], in accordance with previous research, identified two conditions on the wetted flow which are required for the existence of a ventilated flow:

- A zone of low pressure, i.e. pressure lower than the atmospheric pressure, so a pressure gradient can entrain air towards the suction side,
- A separated flow on the suction side, i.e. a recirculation bubble.

These two conditions are necessary for stable ventilation, but not sufficient for the spontaneous transition to ventilated flow, since this requires the air to break through the attached flow with atmospheric pressure at the free surface. This explains

why both flows can be stable under the same conditions. Figure 3 shows an example for a vertical hydrofoil at an angle of attack (yaw) of  $12.5^\circ$ . The wetted flow validates the conditions above and the ventilated flow shows a 33% drop in lift compared to the wetted flow.

Bi-stable flow is a difficulty for the simulation of ventilation: an incomplete analysis of an operational configuration might conclude that a set of conditions is safe because the wetted flow around a foil is stable. However, if this set of conditions is actually bi-stable, a perturbation in a practical case could lead to a ventilated flow, and the foil would not perform as expected. Thus, assessing the risk of ventilation in a bi-stable region through numerical simulation requires first, that the simulation should be able to produce a spontaneous or forced transition from wetted to ventilated flow. And second, when ventilation occurs it must remain stable even in the lower part of the bi-stable range for the angle of attack. The goal of this paper is to investigate these two conditions.

## 2 TEST CASE

This paper investigates the simulation of ventilation for a vertical, surface-piercing hydrofoil that was studied experimentally by Harwood et al. [2, 3]. The present study varies the angle of attack  $\alpha$  for a fixed immersion-based Froude number  $Fn_h = 2.5$ . In the experiments, for  $\alpha$  between  $2.5^\circ$  and  $15^\circ$ , wetted flow was established naturally but ventilated flow could be obtained through a perturbation by a blast of air at the leading edge. The current study instead focuses on natural transition by increasing  $\alpha$  in steps of  $2.5^\circ$  through the bi-stable region until spontaneous ventilation occurs, and then decreasing it until the flow re-attaches to the foil, thus moving along a hysteric cycle (Figure 1). The experiments were conducted in a towing tank at fixed  $\alpha$  for each run, while the carriage was accelerated from zero to the target  $Fn_h$  for that run. The hysteric cycle was therefore along  $Fn_h$  and not  $\alpha$ .

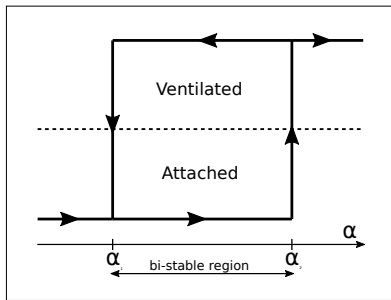


Figure 1: Schematic representation of the hysteric cycle

The symmetrical foil has a chord  $c = 0.279m$  with an ogival fore-body, a rectangular aft-body and a blunt trailing edge. The immersion depth is  $h = c$ . The computational domain is  $6.7m$  wide with the foil centered,  $4.05m$  high with  $3.05m$  water depth and  $9m$  long with the foil at  $3m$  from the front.

The RANS solver used in this study is ISIS-CFD, a two-fluid solver developed by Ecole Centrale de Nantes/CNRS and part of NUMECA International's simulation suite FINE<sup>TM</sup>/Marine. The water surface is represented with a water-air mixture surface capturing model using compressive discretisations, see [4]. Turbulence is modelled with the  $k - \omega SST$  (Menter) model. Adaptive grid refinement is used with a combined free-surface and pressure/velocity Hessian criterion, described in [5]. The Hessian threshold is set at  $0.05m$  ( $\approx 0.18c$ ), the target cell size normal to the free surface is  $c/100$  and the minimum cell size is  $c/500$ . The initial mesh is only refined around the foil, with a wall-resolved boundary condition and  $y^+ < 1$  for the first cells. The flow is solved using a 1<sup>st</sup>-order accurate time-marching algorithm with a time step of  $c/(100U_\infty)$ , during which the refinement procedure is called every 20 steps. Figure 2 shows examples of the meshes.

Two methods were applied to start the computations: (a) increasing the speed of the foil from zero to reach the desired  $Fn_h$ , with  $\alpha$  fixed, and (b) changing  $\alpha$  at fixed speed (and  $Fn_h$ ) from a previous computation. Method (a) was used to start computations from scratch, while method (b) was used to move along the hysteric cycle in  $\alpha$ .

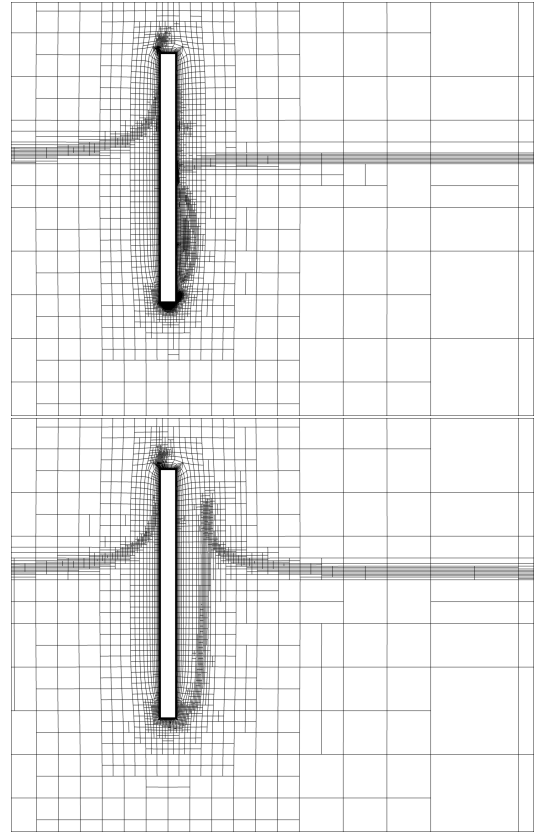


Figure 2: Overview of the mesh adaptation in a transversal cut: wetted (top) and ventilated (bottom) flow at  $\alpha = 20^\circ$ . The mesh is refined around the free surface, in the recirculation bubble (for the wetted flow) and around the tip vortex

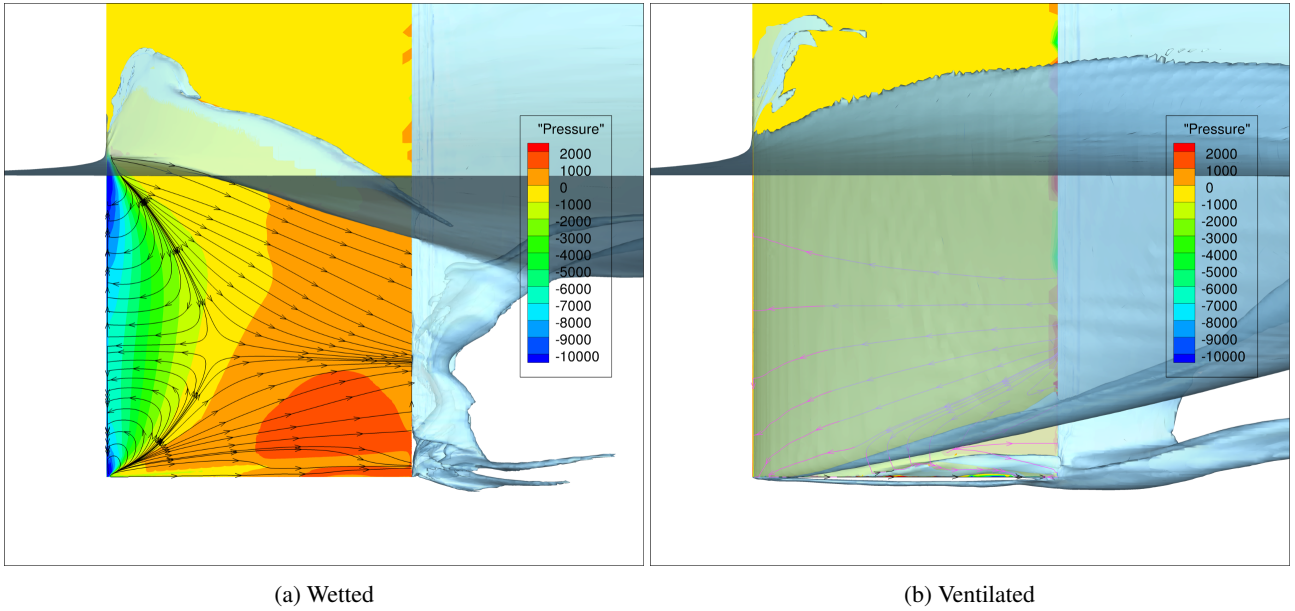


Figure 3: Two flow regimes are stable at  $\alpha = 12.5^\circ$  and  $Fn_h = 2.5$  (pressure, wall streamlines and free surface in a side view of the suction side).

### 3 STEADY FLOWS

Before studying the transition mechanisms that allow the flow to switch from one stable state to another, the steady flow regimes are simulated. Where possible, the results are compared with experiments from [2, 3]. Furthermore, the insight from the visualization of the computed flow fields gives a precise idea of the flow features, allowing for a better understanding of the transition mechanisms later on.

The size of the refined meshes goes from around 4M cells for a ventilated case to 9M cells for a wetted case. Computations were performed on a 20-core Intel Xeon workstation and took between 24 and 48 hours, depending on the size of the adapted mesh.

The wetted flow is shown in Figure 3a and is characterised by a recirculation bubble with subatmospheric pressure covering a part of the suction side. This bubble consists of two vortices flowing one from the top of the leading edge and the other from the bottom of the leading edge, which join together along the immersed span of the foil. Figure 5 compares the extent of the recirculation bubble on the suction side in simulations and experiments, and shows good agreement.

For the wetted flow, a ‘seal’ exists near the free surface: a narrow strip of attached flow at close to atmospheric pressure on the suction side, between the recirculation bubble and the free surface (Figure 3a). This prevents the free surface from breaking and letting air flow into the recirculation bubble via the area of very low pressure at the top of the immersed leading edge. The blunt trailing edge always creates a ventilated cavity in the immediate wake of the foil at  $Fn_h = 2.5$ . The

bottom of the ventilated trailing edge cavity and the tip vortex are unsteady: small air pockets are entrained from the trailing edge by the tip vortex and detach periodically in the wake. This unsteadiness increases with  $\alpha$ .

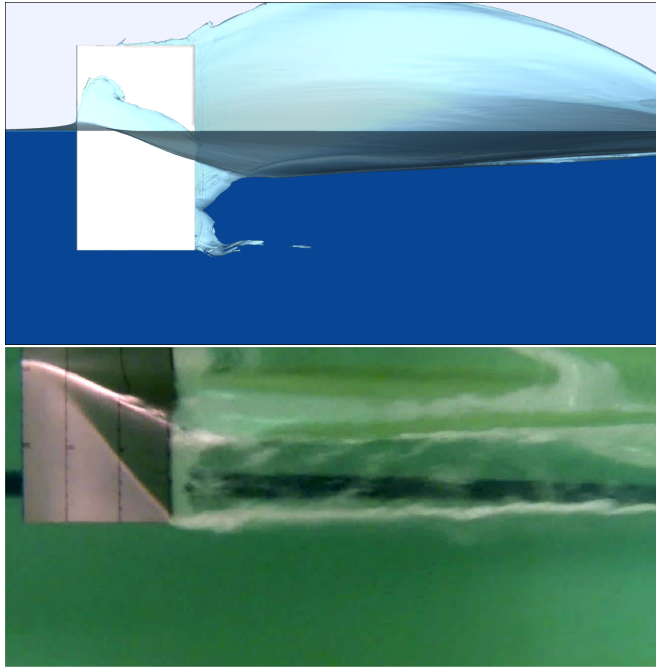


Figure 4: Free surface at  $\alpha = 15^\circ$  for the wetted flow, compared with experiments [3]

Compared with the experiments, the free-surface shape is predicted well (Figure 4), although details such as the bubbly flow in the tip vortex are missing from the simulations.



Figure 5: Comparison between smearing paint drops pattern obtained in the experiments [3] and streamlines obtained by simulation for the wetted flow on the suction side at  $\alpha = 14^\circ$

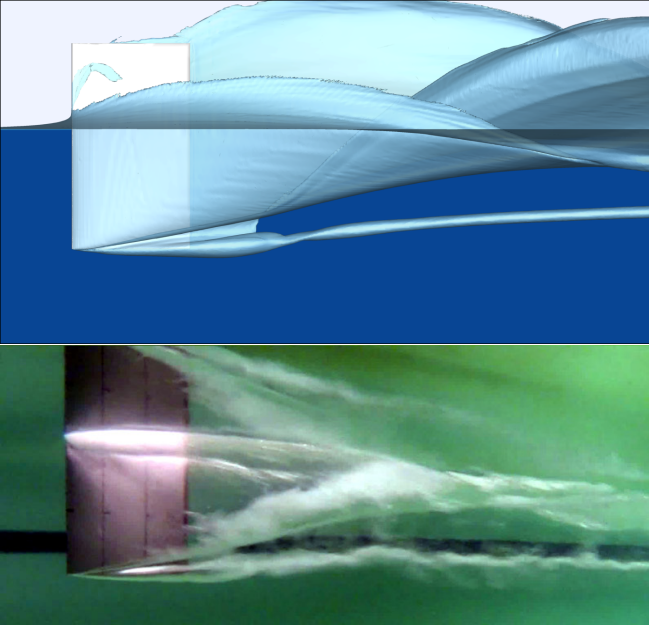


Figure 6: Free surface at  $\alpha = 15^\circ$  for the ventilated flow, compared with experiments [3]

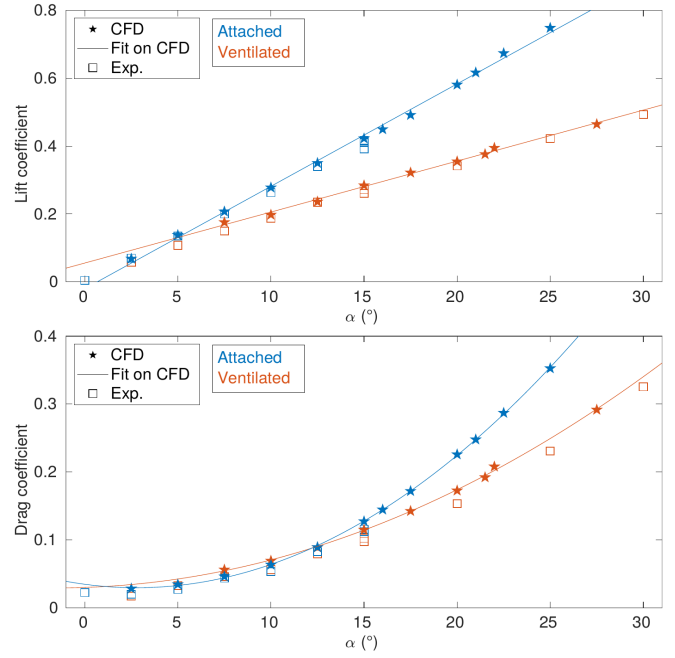


Figure 7: Variation of the lift and drag coefficient: comparison of CFD and experiments from [3]

In the ventilated state, a cavity of air covers the suction side (Figures 3b and 6). The air enters this cavity from above, forms a large recirculation zone on the foil's suction side and exits in the wake. The tip vortex is fully ventilated and entrains a stream of air from the extremity of the foil to the wake. The top of the air cavity is a sheet of water breaking into droplets of water. With the current numerical setup, such droplets are translated into a diffuse low volume fraction cloud which will be described in Section 5. The two sides of the ventilated cavity, coming from the pressure and suction sides, hit each other in the wake, closing the cavity. Their collision creates a spray sheet that is captured well by the simulations.

Figure 7 shows the lift and the drag forces obtained in the simulations, compared with the experimental data. These confirm that both the wetted and the ventilated states are predicted correctly. The evolution of the forces along  $\alpha$  also highlights the hysteretic aspect of the flow, with the two states (wetted and ventilated) being possible for the same configuration. However, the limits of the wetted and ventilated state are not the same as in the experiments: attached flow is observed for much higher angles of attack, while no ventilated flow is produced at the lowest angles. This is due to the transition mechanisms between the two flows, discussed in the next sections.

#### 4 TRANSITION TO A VENTILATED STATE

For the flow to transition from a wetted to a ventilated state, a path needs to open up between the surface and the recirculation bubble, through which air can flow [6]. In the present

case, the main air path runs down the leading edge to the low pressure peak in the bubble (Figure 8). However, in the wetted state (Figure 3a) this path is blocked by the attached flow at ambient pressure along the free surface. To obtain ventilation, this surface seal must be breached.

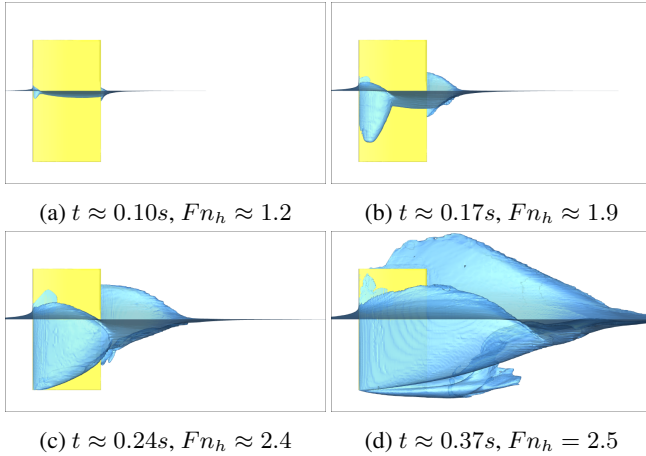


Figure 8: Spontaneous ventilation inception at  $\alpha = 21.5^\circ$ . The acceleration phase is 0.304s long

In the experiments, spontaneous ventilation inception (above  $\alpha = 15^\circ$ ) is attributed to bubbles of air and turbulent vortex cores breaking the free surface at the leading edge [3]. Such flows cannot be simulated with the present free-surface discretisation and RANS turbulence model, so the inception mechanism for the simulations is the full separation of the flow at the top of the leading edge (Figure 8).

The simulations show that apart from the flow model, ventilation inception depends strongly on the path to the steady state. When increasing  $\alpha$  at fixed  $Fn_h = 2.5$  (method (b)), spontaneous ventilation occurs at  $27.5^\circ$ , when unsteady fluctuations of the wake start reaching the foil (Figure 9). However, spontaneous ventilation occurs at angles as low as  $12.5^\circ$ , as opposed to  $15^\circ$  in the experiments, when accelerating slowly from zero speed like in Figure 8 (method (a)). The reason for the difference between the two methods is that at  $Fn_h$  below 2.5, the wave behind the leading edge is shorter but steeper. This means that ventilation inception occurs more easily than at higher speeds. Thus, the inception takes place during the slow acceleration, after which the flow remains in the ventilated state until  $Fn_h = 2.5$  is reached.

Thus, since ventilation transition depends more on *unsteady* – either transient or turbulent – phenomena than on the final steady flow conditions, we conclude that there is little practical interest in the investigation of spontaneous ventilation inception. Nature is rife with perturbations of all types, so the actual ventilation would never appear under the same circumstances as in simulation. It is more relevant to numerically evaluate the risk of ventilation occurring than to simulate actual transitions.

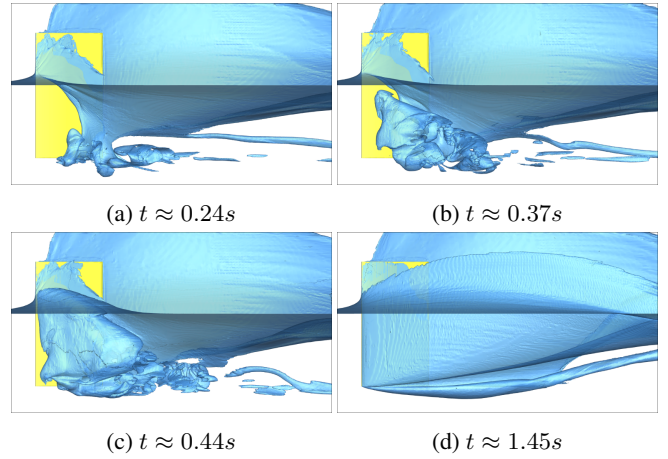


Figure 9: Spontaneous ventilation inception when  $\alpha$  increases from  $25^\circ$  to  $27.5^\circ$  at constant  $Fn_h = 2.5$ . The rotation phase is 0.202s long

To assess the risk of ventilation in a given configuration, we recommend to simulate a big disturbance of the wetted flow, e.g. a sideways acceleration, sufficient to trigger at least a transient ventilated state. The stability of this ventilated flow after the disturbance has stopped determines if the configuration belongs to a bi-stable region. The stability of the wetted flow – i.e. how difficult it is to trigger ventilation – gives an insight into the likeliness of ventilation occurring in practice.

## 5 STABILITY OF THE VENTILATED STATE

Contrary to the inception, it is essential to simulate correctly the stability of the ventilated state, i.e. if it spontaneously returns to a wetted state or not when the angle of attack is decreased. Otherwise, a bi-stable state may be incorrectly considered as free of ventilation risk, which would produce wrong lower boundaries of the bi-stable regions. Assessing the stability requires the study of ventilation elimination.

In the experiments, elimination occurs when lowering  $Fn_h$  at fixed  $\alpha$ . In that case, the ventilation pocket gradually closes from below, with a re-entrant jet on the foil surface rising steeper and steeper until it flows back to the leading edge and closes the ventilated pocket. However when lowering  $\alpha$  at fixed  $Fn_h$  during simulations, ventilation elimination occurs at around  $8^\circ$ , as opposed to the  $2.5^\circ$  suggested by [3]. With  $Fn_h$  staying at 2.5, the re-entrant jet remains on the lower side of the foil. Instead of the ventilation pocket closing from below, the crest of water at the top of the pocket slowly hits the suction side and collapses, closing the air pocket and cutting off the air inflow. Without the inflow, the flow of air into the wake can no longer be sustained. Some air remains for some time in the recirculation zone, but ends up being chased out, leading to a wetted state (Figure 10).

To fully understand how the water crest collapses and closes

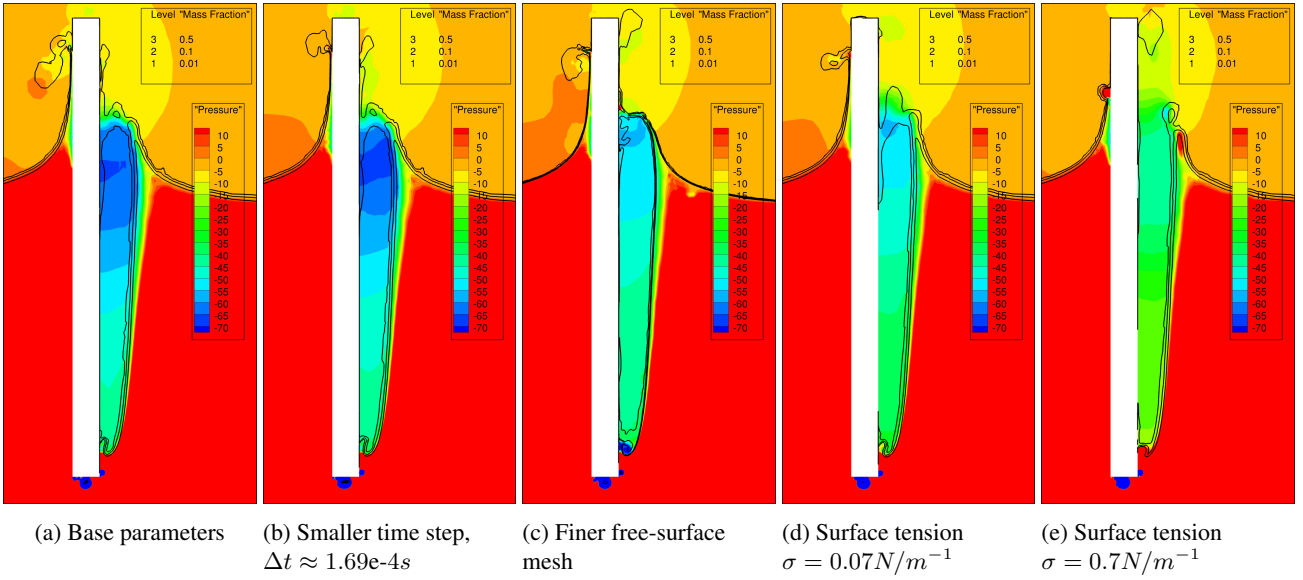


Figure 11: Slice of the ventilated pocket at  $x = 0$  (mid-chord) for  $\alpha = 10^\circ$  and different numerical parameters. The pressure gradient introduced by the diffusion of low water fraction is responsible for the collapse of the air pocket

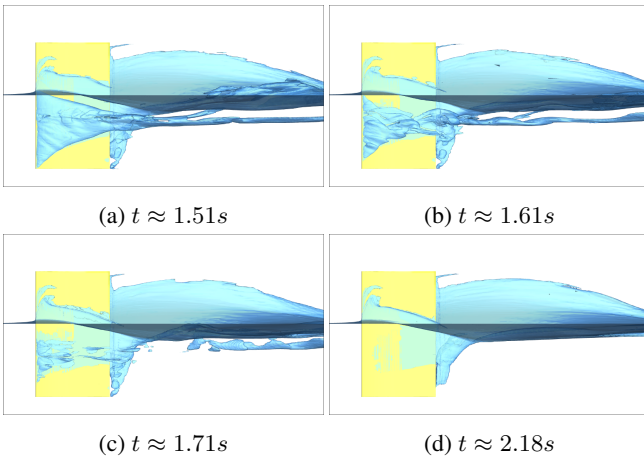


Figure 10: Ventilation elimination at  $\alpha = 7.5^\circ$ .  $\alpha = 10^\circ$  at  $t = 0$ , the rotation to  $7.5^\circ$  is done over  $0.101s$ . A thin layer of air on the suction side is eliminated slowly because the speed is zero on the foil's surface

the air pocket, the pressure and velocity in the air pocket are considered (Figure 11). The top of the water crest over the pocket breaks and creates a bridge to the suction side of the foil. This zone of low water volume fraction prevents air from entering the pocket, further decreasing the naturally lower pressure in the air pocket, which in turn generates high velocities towards the inside of the pocket, pulling the water crest towards the foil. This vicious cycle ends up closing the air pocket from the top. Such a blocking effect might not occur if the breaking of the water crest was not represented by a diffuse low water fraction but by drops of water (which let air pass easily), making this specific issue inherent in the surface-

capturing formulation used.

An indication that the lowered pressure in the ventilated cavity (Figure 11a) is not a physical reality, is the slightly higher lift found in the simulations compared to the experiments for  $\alpha \leq 10^\circ$  (see Figure 7). The order of magnitude of the added lift corresponds to the drop in pressure in the ventilated cavity.

Several attempts have been carried out to solve this problem. Because the compressive volume fraction scheme used in ISIS-CFD [4] is sensitive to the local Courant number, the time step has been reduced. However as Figure 11b shows, even though the local Courant number is divided by 4, the diffusion of the water fraction at the crest does not change. Increasing the mesh refinement at the free surface to get a finer representation of the water-air interface reduces the induced pressure gradient – at the cost of computational speed – but does not remove the low volume fraction bridge (Figure 11c).

Physically, the phenomenon responsible for the breaking of a water sheet into droplets is the surface tension, which tends to minimize the area of the free surface. Thus, a surface tension model, based on [1] but with the surface tension included in the pressure gradient, is tested. This model removes the bridge when using a surface tension 10 times higher than in reality (Figure 11e). However, this changes some other features of the flow and introduces additional numerical problems (e.g. unstable forces created by non-physical pressures on the foil). Using the actual air-water surface tension  $\sigma = 0.07N.m^{-1}$  (Figure 11d) yields similar results to refining the free surface (Figure 11c) in terms of the pressure gradient, while reducing the amount of water arriving on the foil surface significantly.

As a follow-up, the rotation from  $10^\circ$  to  $7.5^\circ$  is repeated with

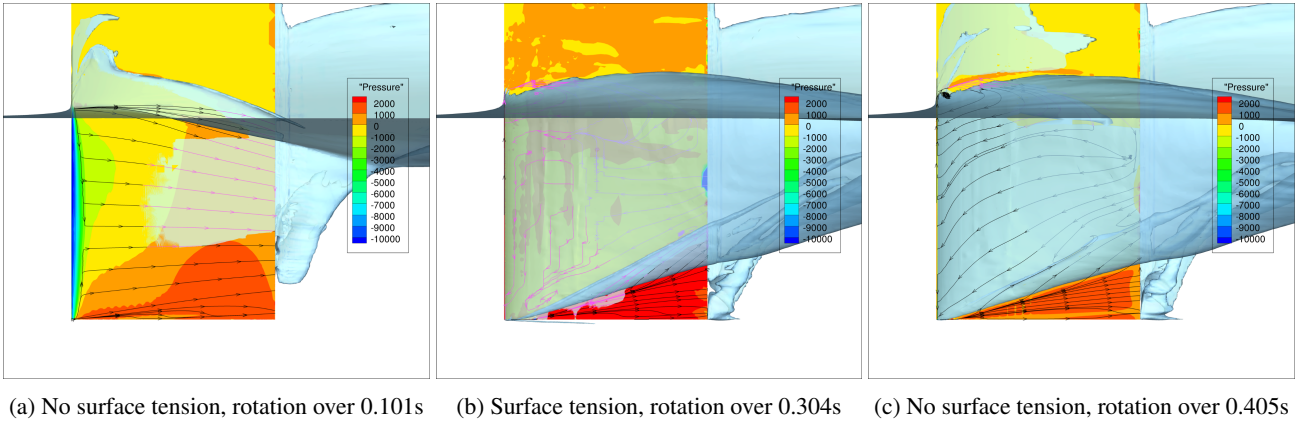


Figure 12: Both adding a surface tension model and slowing the rotation rate (coming from  $10^\circ$ ) prevents the flow from rewetting at  $\alpha = 7.5^\circ$

the actual air-water surface tension. While the flow without surface tension reattaches (Figure 12a, see also Figure 10), the surface tension model maintains a stable ventilated state (Figure 12b). However, the rotation rate to  $7.5^\circ$  was reduced for this computation and it was later found out that a sufficiently slow rotation rate on its own is enough to prevent the flow from reattaching (Figure 12c). But in this last computation a sheet of water is present on the foil, which is removed by the surface tension model. This may be an indication that the surface tension reduces the risk of reattachment.

Furthermore, the surface tension model reduces the suction in the ventilated pocket, compared to the computation without surface tension (Figure 13). However, this image shows that although less water is impacting on the foil, the low volume-fraction ‘bridge’ between the water crest and the foil is still present. It is likely that this bridge will eliminate the ventilating pocket if the angle of attack is reduced even further.

Thus, while the motion history of the foil must once again be taken into account, the two tests indicate that the physical and numerical modelling of the water crest is a factor in the ventilation elimination. However, only the simulation with an artificially high surface tension (Figure 11e) produces the straight crest which is observed in images from the experiments. Also, the irregular surface pressure in Figure 12b is problematic. These are indications that the current surface tension model is ill adapted for the diffused low volume fractions that appear in the wave crest. A more detailed study of the surface tension and surface-capturing models for this flow is planned for future work.

## 6 CONCLUSION

This paper studies the inception and stability of ventilation in bi-stable conditions. More specifically, a bi-stable range of the angle of attack for a vertical surface-piercing hydrofoil at fixed travel speed is discussed in depth. The goal of the

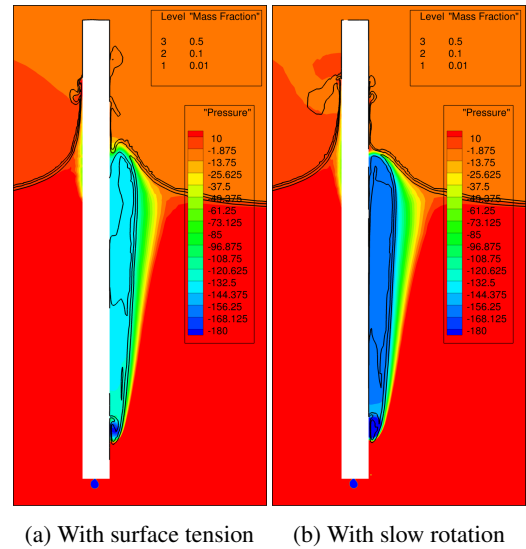


Figure 13: Slice of the ventilated pocket at  $x = 0$  (mid-chord) for  $\alpha = 7.5^\circ$

study is to assess the capacity of RANS simulation with two-fluid surface-capturing to predict the two flow states and the transitions between them.

First, the different features of each flow regime are exposed: a recirculation bubble, a tip vortex, subatmospheric pressures, and complex free-surface topology. For the free surface position and the forces, good agreement is found between simulations and experiments.

It is shown that spontaneous inception depends on the path to the steady state. Slowly accelerating the flow from rest produces ventilation inception through the rupture of the surface seal at the leading edge, while increasing the angle of attack at fixed Froude number causes a transition starting from the ventilated trailing edge. This shows that transient mechanisms are responsible for the inception of ventilation and that transi-

tion to ventilation is always likely to occur through (random) perturbations whenever the conditions belong to a bi-stable region. Thus, to assess the risk of ventilation occurring, it is more relevant to provoke ventilation by artificial perturbation and to consider its stability, than to simulate spontaneous inception.

At low angles of attack, the simulated ventilation is eliminated numerically through a choking phenomenon: the water crest on top of the ventilated cavity breaks and impacts the suction side of the foil. This cuts off the air flow into the cavity and decreases the pressure in the cavity, which triggers the collapse of the cavity. The numerical transition is different from the experimental results, where the cavity closes from the bottom. Adding a surface tension model raises the pressure in the ventilated cavity, but is insufficient to compress the low volume fraction diffusion. However, this test confirms that the mechanism of ventilation elimination depends on the detailed physical and numerical modelling of the water sheet which forms the edge of the ventilating pocket.

## 7 ACKNOWLEDGEMENTS

This work was granted access to the HPC resources of the IDRIS computing centre under the allocation 2018/2019-A0052A01308 made by GENCI (Grand Equipement National de Calcul Intensif). We thank Prof. Harwood and his co-authors for the use of their experimental results.

## REFERENCES

- [1] J. U. Brackbill, D. B. Kothe, and C. Zemach. A continuum method for modeling surface tension. *J Comp Phys*, 100:335–354, 1992.
- [2] C. M. Harwood, K. A. Brucker, F. M. Montero, Y. L. Young, and S. L. Ceccio. Experimental and numerical investigation of ventilation inception and washout mechanisms of a surface-piercing hydrofoil. In *30th ONR Symposium on Naval Hydrodynamics*, Hobart, Tasmania, 2014.
- [3] C. M. Harwood, Y. L. Young, and S. L. Ceccio. Ventilated cavities on a surface-piercing hydrofoil at moderate Froude numbers: cavity formation, elimination and stability. *J Fluid Mech*, 800:5–56, 2016.
- [4] P. Queutey and M. Visonneau. An interface capturing method for free-surface hydrodynamic flows. *Comput Fluids*, 36(9):1481–1510, November 2007.
- [5] J. Wackers, G. B. Deng, E. Guilmineau, A. Leroyer, P. Queutey, M. Visonneau, A. Palmieri, and A. Liverani. Can adaptive grid refinement produce grid-independent solutions for incompressible flows? *J Comput Phys*, 344:364–380, 2017.

- [6] Y. L. Young, C. M. Harwood, F. Miguel Montero, J. C. Ward, and S. L. Ceccio. Ventilation of lifting bodies: Review of the physics and discussion of scaling effects. *Appl Mech Rev*, 69(1):010801:1–38, 2017.

## 8 AUTHORS' BIOGRAPHY

**M. Charlou** is a Ph.D. student in Fluid Dynamics at LHEEA Lab, ECN/CNRS. His current work as a Ph.D. student revolves around Wind-Assisted Ship Propulsion, but his Master's Degree thesis was focused on the numerical simulation of bi-stable ventilation around surface-piercing hydrofoils using CFD.

**J. Wackers** is a researcher at LHEEA Lab, ECN/CNRS. He obtained his Ph.D. in numerical aerodynamics at Delft University of Technology in 2007. Since then, he has worked on the study of automatic mesh adaptation for hydrodynamic flow simulation.

**G.B. Deng** is a researcher at LHEEA Lab, ECN/CNRS. In 1989 he obtained his Ph.D. of Fluid Dynamics and Heat Transfer of University of Nantes. His main research themes are in the context of Computational Fluid Dynamics (CFD) such as turbulence model implementation and overset algorithms.

**E. Guilmineau** is a CNRS Researcher at LHEEA Lab, ECN/CNRS. In 1995 he obtained his Ph.D. of Fluid Dynamics and Heat Transfer of University of Nantes and entered CNRS as Research Scientist in 1996. His main research themes are in the context of Computational Fluid Dynamics (CFD) such-simulate as turbulence model implementation, in particular the hybrid RANS-LES models.

**A. Leroyer** is assistant professor at the LHEEA lab. of Centrale Nantes since 2005. His main research topic in the METHRIC group is focused on Fluid-Structure Interaction.

**P. Queutey** is a CNRS Researcher at LHEEA Lab, ECN/CNRS. In 1989 he obtained his Ph.D. of Fluid Dynamics and Heat Transfer of University of Nantes and entered CNRS as Research Scientist in 1990. His main research themes are in the context of Computational Fluid Dynamics (CFD) with the development of numerical schemes for viscous incompressible flows with specific treatments of interface capturing method suitable for sharp prediction of free-surface flows with application to fully unstructured grids for complex geometries.

**M. Visonneau** obtained in 1980 an Engineer's diploma and the diploma of Advanced Naval Architecture in 1981 from Centrale Nantes. In 1985, he got a PhD of Fluid Dynamics and Heat Transfer of the University of Nantes and entered the National Center for Scientific Research (CNRS) as research associate. He was the head of the CFD department of the Fluid Mechanics Laboratory (Centrale Nantes) from 1995

to 2012. In 2001, he defended his Habilitation to supervise Research and was promoted research director at CNRS in 2006. He has supervised more than 20 PhD thesis. He is a member of the Steering Committee of the International Workshop on CFD in Ship Hydrodynamics since 2005. He was awarded the 2nd Cray prize for CFD in 1991 and 30th Georg Weinblum lecturer in 2007. In 2006, he built a partnership with NUMECA Int. which gave birth to FINE/Marine and is now in charge of the scientific management of this worldwide distributed software.